1   **Article Type**: *Methods* contribution to *Ecology Letters*

2   **Title:** Relative species abundance and population densities of the past; developing multi-

3   species occupancy models for fossil data

4

5   **Running head:** Relative abundance occupancy model

6   **Authors:**

7   Trond Reitan (trond.reitan@ibv.uio.no, Natural History Museum, University of Oslo,

8   Norway)

9   Torbjørn Ergon (t.h.ergon@ibv.uio.no, Centre for Ecological and Evolutionary Synthesis,

10   Department of Biosciences, University of Oslo, Norway)

11   Lee Hsiang Liow* (l.h.liow@nhm.uio.no, Natural History Museum, University of Oslo,

12   Norway)

13   *corresponding author

14   **Key words:** occupancy models, relative abundance, Bayesian, sites, subsamples, fossil

15   record

24   **Word count** in main text = 4996; **No. references** = 34; **No. figures** = 6

Abstract

The number of individuals of species within communities varies, but estimating abundance, given incomplete and biased sampling, is challenging. Here, we describe a new occupancy model in a hierarchical Bayesian framework with random effects, where multi-species occupancy and detection are modeled as a means to estimate relative species abundance and relative population densities. The modelling framework is suited for occupancy data for temporal samples of fossil communities with repeated sampling including multiple species with similar preservation potential. We demonstrate our modelling framework using a fossil community of benthic organisms to estimate changing relative species abundance dynamics and relative population densities of focal species in 9 (geological) time-intervals over 2.3 million years. We also explored potential explanatory factors (paleoenvironmental proxies) and temporal autocorrelation that could provide extra information on unsampled time-intervals. The modelling framework is applicable across a wide range of questions on species-level dynamics in (palaeo)ecological community settings.

(148 Words)

Introduction

Understanding past and contemporary patterns and dynamics of populations and communities requires robust estimates of variation in abundance of organisms (Williams *et al.* 2002; Sutherland *et al.* 2013). While it is notoriously difficult to estimate absolute population sizes or densities due to the imperfect detection of individuals (Schwarz & Seber 1999), it is generally much easier to estimate relative differences/changes in population sizes/densities (Williams *et al.* 2002). Fortunately, such relative estimates are often sufficient for ecological inference. For example, community ecologists have long been interested in explaining distributions of relative species abundance (RSA; i.e., the abundance of a species relative to the abundance of other species) in communities (Fisher *et al.* 1943; MacArthur & Wilson 1967). Likewise, it is often sufficient to model relative changes in population density (hereafter 'relative population density' (RPD)) over time (Royama 1992; Caswell 2001) due to the multiplicative nature of population dynamics.

While contemporary ecological data and fossil data reflect ecological and evolutionary processes at vastly different time-scales, sampling strategies and data structure may be similar. Like contemporary ecological data, fossil data often consist of detection records of species. Fossil records are often associated with geological formations (time-intervals) of different ages, where low or zero detection frequencies in certain formations may be due to low (then) extant population densities and/or low preservation probabilities. When detection and non-detection of focal species in replicated samples have been recorded, it is possible to estimate both occupancy and the probability of detection, given occupancy (MacKenzie *et al.* 2002). Over the past decades a rich literature on such 'species occupancy models' has emerged (King 2014; MacKenzie *et al.* 2017). Originally, these models were developed to estimate the probability of true species presence, e.g. as a function of habitat variables. Later developments also linked detection probabilities to species abundance (Royle

3

65   & Nichols 2003). Multi-species expansions of these models have facilitated studies of

66   community composition and species richness (Dorazio *et al.* 2006; Yamaura *et al.* 2011;

67   Iknayan *et al.* 2014; Devarajan *et al.* 2020).

68   With an appropriate sampling design, occupancy models may be fitted to fossil data to

69   address paleoecological questions (Liow 2013). Here, we develop a multi-species occupancy

70   model, tailored for fossil occupancy data, aimed at estimating temporal patterns (over

71   millions of years) of relative species abundance (RSA) and relative population density

72   (RPD). As is typical for fossil data, preservation also influences detection probability, and the

73   preservation can vary substantially among formations (Behrensmeyer *et al.* 2000). One way

74   of tackling temporal variation in preservation is by incorporating random effects for

75   formations. By incorporating data from multiple species, we aim to reduce the influence of

76   preservation on abundance estimates by "filtering out" formation-specific random effects on

77   detection probability common to all species. Importantly, random effects also allow us to

78   estimate formation-specific RSA and RPD when data consists of multiple samples (sites) and

79   sub-samples (replicates). In addition to formation-specific random effects, we also use those

80   that capture the dynamics of individual species. All of these random effects allow us to

81   "borrow strength" across species (e.g. Zipkin *et al.* 2010).

82   Using simulated data, we explore if ecological dynamics can be accurately inferred

83   using our model, and then apply this model to a dataset of marine invertebrates (cheilostome

84   bryozoans) that attach to hard substrates (shells) over 9 time-intervals (geological formations)

85   spanning 2.3 million years from a marine basin in New Zealand. We discuss the general

86   utility of our model in paleoecological settings, and suggest venues for further development.

87

88   **Materials and methods**

89   *Study system*

90   The empirical example we use is a community of fossilized benthic organisms found in the

91   Wanganui Basin (Carter & Naish 1998; Proust *et al.* 2005; Pillans 2017). We examined

92   subsamples (= shells) in 119 sites within 9 geological formations rich in fossil marine

93   deposits representing time-intervals from 2.29 to 0.30 million years ago (Fig. 1), in which the

94   number of shells varied between 30-50 (Table S1). By assuming that species' abundances in

95   sampled sites are representative for the region at the time they were preserved, we can make

96   regional estimates for each time-interval. We tabulated the observed presence of any

97   fossilized individuals of three focal species namely *Antharcthoa tongima*, *Escharoides*

98   *excavata* and *Arachnopusia unicornis* (Fig. S1) on each shell. There is ample among-

99   formation, within-formation and among-species variation in the detection ratio, i.e. the

100   number of shells with focal species of encrusting bryozoans observed divided by the total

101   number of shells examined (Fig. S2). We also introduce a fourth "species", the superspecies,

102   which represents all other encrusting bryozoan species in the community, excluding the three

103   focal species. In doing so, we can utilize observations from other species in the same

104   community without collecting detailed species-level data in a species-rich system, to improve

105   parameter estimates (see Model Description). In addition, by including the superspecies,

106   estimated species abundances will be relative to all bryozoan species, rather than only the

107   sum of the included focal species. Since the formations were chosen because they are known

108   to harbor bryozoans, our superspecies is assumed to always be present, i.e. occupancy

109   probability=1. In other applications, a superspecies can be excluded or the occupancy

110   probability of the superspecies can be estimated within the model.

111

112 *Model description*

113 Our main objective is to estimate the temporal (i.e. formation-to-formation) dynamics of RSA

114 and RPD (we refer to both as "relative abundance" for short until section 6) for each focal

115 species using detection/non-detection observations on subsamples (shells in our empirical

116 example) from different sites (Fig.1, Fig. S1). We begin with a standard occupancy model,

117 where the probability that a species occupied a given site i.e. the occupancy probability, Ψ,

118 and the probability that a subsample has at least one observation of the focal species, given

119 occupancy, i.e., the detection probability, p. The probability that a species is found on a given

120 subsample is thus Ψp, where Ψ operates on the site-level while p operates on the subsample-

121 level. The occupancy and detection probabilities will be functions of various parameters and

122 random effects, and can be specific to the site i belonging to a specific time-interval, f, and

123 the species, s. Thus, we write $\Psi_{i,s}(\theta)$ and $p_{i,s}(\theta)$ for the occupancy and detection

124 probabilities respectively, where θ is the set of top level parameters and random variables of

125 the model in question (Fig. 2). The relative abundances for each focal species will be derived

126 from these two sets of probabilities.

127 We proceed in a step-wise fashion, adding complexity to a standard occupancy model

128 until it has enough elements for relative abundance estimates. We do this for three reasons.

129 The first is to put focus on each of the model components. Second, because MCMC

130 convergence was achieved only when we used the parameter estimates from a simpler model

131 as the starting points for the next, more complex model. Thirdly, because we wanted to

132 justify adding model complexity, using the Bayes factor as measure of evidence (Jeffreys

133 1998).

134

135   1. The basic occupancy model for number of detections per site

136   In a basic occupancy model (MacKenzie *et al.* 2002), $y_{i,s}$ is the number of subsamples at site

137   i with observations of species s, is a zero-inflated binomial random variable.

138    $$y_{i,s} \sim zbin\left(N_i, p_{i,s}(\theta) = \text{logit}^{-1}(\beta_s), \Psi_{i,s}(\theta) = I(s = S) + I(s < S)\text{logit}^{-1}(\alpha_s)\right) \qquad (1)$$

139   N_i is the total number of subsamples examined at site *i*. *I()* stands for the indicator

140   function, which takes value 1 when the statement inside is true and 0 if false. The

141   unconditional probability of detection is $p_{i,s}(\theta)\Psi_{i,s}(\theta)$. We express both occupancy and

142   detection probabilities using a logit-transform, i.e. $\text{logit}(r) \equiv \log\left(\frac{r}{1-r}\right)$, where r is a

143   probability, for the convenience of expanding the model (see next sections). The two

144   parameters, α_s and β_s, (Fig. 2) give regional (i.e. within the Wanganui Basin in our

145   application) occupancy and detection probabilities for each species, regardless of time-

146   interval (formation). The parameter set is $\theta = \{\alpha_1, \cdots, \alpha_{S-1}, \beta_1, \cdots, \beta_S\}$, where *S* is the

147   number of species (focal species plus superspecies). The subscript *i* is included for clarity

148   although sites are not considered in this section. $\alpha_{s=S}$ does not appear, as we assume that the

149   superspecies is always present.

150

151   2. Including site-dependent random effects for number of detections per site through

152   overdispersion

153   Variation in abundance among sites is expected in natural systems. Since detection is linked

154   to true abundance, the detection probability of a given species is expected to fluctuate from

155   site to site. Fossil preservation can also influence detection probabilities on the site-level.

156   Observations in our dataset consists of one summary data point per site (tabulated from the

157   subsample replicates) per species, and we thus use overdispersion for modelling instead of a

158   per observation random effect (Harrison 2014). This is because including random effects for

159   each of these would radically and unnecessarily increase model complexity. Hence, to

160 facilitate extensive simulations, we use the beta-binomial distribution which has an analytical

161 expression, namely

162 $$P_{\beta bin}(y|n,p,\kappa)=\frac{\Gamma(n+1)\Gamma\left(y+\frac{p}{\kappa}\right)\Gamma\left(n-y+\frac{1-p}{\kappa}\right)\Gamma\left(\frac{1}{\kappa}\right)}{\Gamma(y+1)\Gamma(n-y+1)\Gamma\left(n+\frac{1}{\kappa}\right)\Gamma\left(\frac{p}{\kappa}\right)\Gamma\left(\frac{1-p}{\kappa}\right)},$$ (2)

163 where y out of n is the outcome, p the detection probability and κ the overdispersion

164 parameter where $\kappa = 0$ means no overdispersion (see SI for details). This specifies the

165 distribution of detections given occupancy. Thus, the zero-inflated (un-conditioned on

166 occupancy) beta-binomial distribution is:

167 $$P_{z\beta bin}(y|n,p,\kappa,\Psi)=(1\text{-}\Psi)I(y = 0) + \Psi\frac{\Gamma(n+1)\Gamma\left(y+\frac{p}{\kappa}\right)\Gamma\left(n-y+\frac{1-p}{\kappa}\right)\Gamma\left(\frac{1}{\kappa}\right)}{\Gamma(y+1)\Gamma(n-y+1)\Gamma\left(n+\frac{1}{\kappa}\right)\Gamma\left(\frac{p}{\kappa}\right)\Gamma\left(\frac{1-p}{\kappa}\right)}$$ (3)

168 where Ψ is the zero-inflation and the likelihood is:

169 $$y_{i,s} \sim z\beta bin\left(N_i, p_{i,s}(\theta) = \text{logit}^{-1}(\beta_s), \kappa_s, \Psi_{i,s}(\theta) = I(s = S) + I(s < S)\text{logit}^{-1}(\alpha_s)\right)$$ (4)

170   κ_s describes the species-dependent overdispersion, while the other terms are as in Eqn

171 1. The parameter set is now $\theta = \{\alpha_1, \cdots, \alpha_{S-1}, \beta_1, \cdots, \beta_S, \kappa_1, \cdots, \kappa_S\}$. The detection and

172 occupancy probabilities depend on the identity of the time-interval that the site belongs to,

173 rather than the site itself, as the beta-binomial distribution accounts for the overdispersion

174 among sites. At this point no time-interval dependency has been added.

175

176 3. Including species- and formation-dependent random effects

177 We now introduce temporal dynamics by using time-interval-dependent random effects that

178 are species-independent, i.e. they summarize dynamics common to all species in the

179 community. For the detection probability, the random effects imply fluctuations in the

180 preservation as well as in average abundance of all species in the community. For occupancy,

181 the random effects allow fluctuations in the overall presence of the set of species in question.

182 The time-intervals with richer data can thus inform estimates for those with sparser data. The

183 model is now:

184 $$y_{i,s} \sim z\beta bin\left(N_i, p_{i,s}(\theta) = \text{logit}^{-1}(\beta_s + u_{f(i)}), \kappa_s, \Psi_{i,s}(\theta) = I(s = S) + I(s < \right.$$

185 $$\left. S)\text{logit}^{-1}(\alpha_s + v_{f(i)})\right)$$ (5a)

186 $$u_f \sim N(0, \sigma_u^2), v_f \sim N(0, \sigma_v^2),$$ (5b)

187 where $f(i)$ is the time-interval that site i belongs to, u_f and v_f are the new time-interval-

188 dependent random effects and σ_v and σ_u are the standard deviations of these effects for

189 detection and occupancy respectively. Now, $\theta =$

190 $\{\alpha_1, \cdots, \alpha_{S-1}, \beta_1, \cdots, \beta_S, \kappa_1, \cdots, \kappa_S, \sigma_u, \sigma_v, u_1, \cdots, u_F, v_1, \cdots, u_F\}$, where F is the number of

191 time-intervals.

192   While Eqn 5 does allow for dynamics due to time variations in the whole set of

193 species in the region, the species probabilities are in sync. To facilitate dynamics that permit

194 fluctuations in the relative species-dependent abundances, we need random effects that

195 depend on species and formation combinations. When doing so, we have:

196 $$y_{i,s} \sim z\beta bin\left(N_i, p_{i,s}(\theta) = \text{logit}^{-1}(\beta_s + u_{f(i)} + \varepsilon_{f(i),s}), \kappa_s, \Psi_{i,s}(\theta) = I(s = S) + \right.$$

197 $$\left. I(s < S)\text{logit}^{-1}(\alpha_s + v_{f(i)} + \delta_{f(i),s})\right)$$ (6a)

198 $$u_f \sim N(0, \sigma_u^2), v_f \sim N(0, \sigma_v^2), \delta_{f,s} \sim N(0, \sigma_{\delta,s}^2), \varepsilon_{f,s} \sim N(0, \sigma_{\varepsilon,s}^2)$$ (6b)

199 where $\varepsilon_{f,s}$ and $\delta_{f,s}$ are the new time-interval- and species-dependent random effects and $\sigma_{\varepsilon,s}$

200 and $\sigma_{\delta,s}$ are the standard deviations of these effects, for detection and occupancy,

201 respectively. As $p_{i,s}$ and $\Psi_{i,s}$ only depend on sites in the time period, f, we label them as $p_{f,s}$

202 and $\Psi_{f,s}$ in the following sections.

203   The parameter set is now $\theta = \{\alpha_1, \cdots, \alpha_{S-1}, \beta_1, \cdots, \beta_S, \kappa_1, \cdots, \kappa_S, \sigma_u, \sigma_v,$

204 $\sigma_{\delta,1}, \cdots, \sigma_{\delta,S-1}, \sigma_{\varepsilon,1}, \cdots, \sigma_{\varepsilon,S}, u_1, \cdots, u_F, v_1, \cdots, u_F, \delta_{1,1}, \cdots, \delta_{F,S}, \varepsilon_{f,s}, \cdots, \varepsilon_{F,S}\}$. We choose

205 independent and wide priors for each parameter (see SI section "Prior distribution for the full

206 model"). All positive-valued parameters including the standard deviations and

207 overdispersion parameters are log-transformed so that on re-parametrization, they fall on the

208 real number line. With 3 species and one superspecies we now have *20 (5×S)* top level

209 parameters and 81 (*(2S+1)×F*) random variables (Eqn 6b). We call Eqn 6 the "full model",

210 since it has all the necessary components for estimating relative abundance dynamics (Fig. 2),

211 which we detail in section 6.

212

213 4. A step-wise approach for improving estimation

214 Because the full model is fairly complex and required hierarchically arranged random effects,

215 we utilized Markov chain Monte Carlo (MCMC) sampling for inference (SI section "MCMC

216 for statistical inference"). We used common estimated parameter values from a simpler

217 model when starting a more complex model, in a step-wise fashion (i.e. from Eqn 1 to 4, 5,

218 then 6) as preliminary analyses often failed when starting from a random place in the

219 parameter space. In doing so, we also tested if each increasingly complex model explained

220 the data better, using Bayes factors.

221

222 5. Incorporating explanatory variables

223 We expanded Eqn 6 by including temporal explanatory variables – in our empirical example

224 pertaining to paleoclimate, as well as auto-correlated processes by using an Ornstein–

225 Uhlenbeck process (SI sections "Model expansions that include explanatory variables" and

226 "Introducing correlations in the random effects") although these results not detailed in the

227 main text. Our motivation for examining and testing these expansions was to predict relative

228 abundances in unmeasured time-intervals with more precision than just using the time-

229 interval-independent median values derived from α_s and β_s. We impose a quadratic term for

230 our explanatory variables (on detection probability, occupancy probability or both) as each

231 species should thrive at an different optimal climate, with a given tolerance width. We use

232   two related but different paleoclimate proxies, namely the global $\partial^{18}O$ data (data from

233   Lisiecki & Raymo 2005) and the North Atlantic magnesium/calcium (Mg/Ca) ratios (data

234   from Sosdian & Rosenthal 2009), both based on measurements from benthic foraminiera, as

235   explanatory variables. These contain complex signals of sea temperature, ice-volume and sea-

236   level changes, all of which potentially affect both the population growth rates (through

237   optimal temperatures and the availability of substrate species) and detection probabilities

238   (through sea-level changes) of our focal species. Whether other empirical applications of will

239   benefit from such model extensions is context-dependent.

240

241   6. Estimating relative species abundance (RSA) and relative population densities (RPD)

242   Detection entails observing a species that is present. In typical fossil data, detection

243   requires preservation and successful sampling and taxonomic identification of fossilized

244   organisms. Preservation and hence taxonomic identifiability is often strongly associated with

245   the formation the sample belongs to (Behrensmeyer *et al.* 2000). For the purpose of

246   estimating RSA and RPD, we introduce corrected detection probabilities $p_{f,s}^*(\theta) \equiv$

247   $\text{logit}^{-1}(\beta_s + \varepsilon_{f,s})$, where the purely time-interval-dependent random factors, u_f, are

248   subtracted from the detection probability estimates. This is done with the assumption that the

249   $u_{f(i)}$ terms are mainly affected by the preservation rather than common biological dynamics

250   among species. For our empirical data, preservation is unlikely to affect the time-interval-

251   dependent random factors for occupancy, v_f, thus we assume $\Psi_{f,s}^* \equiv \Psi_{f,s}$. When detection

252   probabilities are low, moderate correlations between detection and occupancy probabilities in

253   the joint posterior distribution could mean that preservation dynamics influenced inferred

254   occupancy probabilities. However, we expect that these indirect effects on such inferred

255   occupancy probabilities to be small compared to common occupancy dynamics.

256   We link the average observable abundance per subsample given occupancy, $\lambda_{f,s}$, to

257   the corrected detection probability. Assuming a point process, $p^*_{f,s}$ is then given by the

258   Poisson distribution:

259     $p^*_{f,s} = P(number\ of\ preserved\ colonies > 0) = 1 - e^{-\lambda_{f,s}}.$ (7)

260   We can hence derive $\lambda_{f,s}$ from an estimate of $p^*_{f,s}$ (main analyses) or derive $p^*_{f,s}$ from

261     $\lambda_{f,s}$ (simulations and SI). Breaking the Poisson distribution assumption due to overdispersion

262   of number of colonies per subsample, only imperceptibly (in our case) affect the abundance

263   estimates much (see SI). Note that Yamaura *et al.* (2011) assumed detection to be the result

264   of sampling from a binomial distribution and the Poisson distribution is a limit of the

265   binomial distribution and Eqn 7 is in fact equivalent to Eqn 1 in Yamaura *et al.* (2011), given

266   a re-parametrization.

267   While we subtract the random factors representing the common preservation

268   dynamics in detection, the average preservation rate over time is unknown. Thus, is a

269   proportionality coefficient, $k_{f,s}$, between the average true and observable abundance per

270   subsample given occupancy, such that

271          $\lambda_{f,s} = k_{f,s}\Lambda_{f,s},$ (8)

272   where $\Lambda_{f,s}$ is the average true abundance per subsample.

273   We first assign both species- and time-interval dependency on $k_{f,s}$ to make explicit

274   the assumptions we later use. In an ideal world, our subtraction of the effects of preservation

275   dynamics when constructing $p^*_{f,s}$ makes the proportionality coefficient both species- and

276   time-interval-independent, i.e. $k_{f,s} = k$.

277   The average true abundance per subsample (unconditioned on occupancy) is;

278     $A_{f,s} = \Psi^*_{f,s}\Lambda_{f,s} = \Psi_{f,s}\lambda_{f,s}/k_{f,s}.$ (9)

279   We can now define the relative species abundance (RSA) as the true abundance per

280   subsample of a species normalized to the sum over all species of a given time-interval ($R_{f,s}$).

281   Under the assumption that preservation is the same for all species in question and that

282   nothing else affects $k_{f,s}$, then the proportionality coefficients will be species-independent, i.e.

283    $k_{f,s} = k_f$. k_f then drop outs when calculating the RSA:

284    $$R_{f,s} \equiv \frac{A_{f,s}}{\sum_{s'=1}^{S} A_{f,s'}} = \frac{\Psi_{f,s}\lambda_{f,s}/k_f}{\sum_{s'=1}^{S} \Psi_{f,s'}\lambda_{f,s'}/k_f} = \frac{\Psi_{f,s}\lambda_{f,s}}{\sum_{s'=1}^{S} \Psi_{f,s'}\lambda_{f,s'}} = \frac{\Psi_{f,s}\log(1-p_{f,s}^*)}{\sum_{s'=1}^{S} \Psi_{f,s'}\log(1-p_{f,s}^*)} \quad (10)$$

285   For an alternative modelling approach, built-up from the average observable

286   abundance per subsample given occupancy, $\lambda_{f,s}$, rather than detection probabilities, see SI

287   "Description of the abundance-focused model".

288   We define the relative population density (RPD), $Q_{f,s}$, as the true abundance for the

289   species at a given time interval relative to the true abundance of the same species averaged

290   over all time intervals. We normalize $Q_{f,s}$ to the temporal mean rather than to a specific time-

291   interval (e.g. the first available), as it is less sensitive to uncertainty and estimates near zero.

292   As long as the proportionality coefficients are independent of time interval, $k_{f,s} = k_s$, we can

293   relate this to observed quantities such that:

294    $$Q_{f,s} \equiv \frac{A_{f,s}}{\frac{1}{F}\sum_{f'=1}^{F} A_{f',s}} = \frac{\frac{\Psi_{f,s}\lambda_{f,s}}{k_s}}{\frac{1}{F}\sum_{f'=1}^{F} \frac{\Psi_{f',s}\lambda_{f',s}}{k_s}} = \frac{\Psi_{f,s}\lambda_{f,s}}{\frac{1}{F}\sum_{f'=1}^{F} \Psi_{f',s}\lambda_{f',s}} = \frac{\Psi_{f,s}\log(1-p_{f,s}^*)}{\frac{1}{F}\sum_{f'=1}^{F} \Psi_{f',s}\log(1-p_{f,s}^*)}. \quad (11)$$

295        $Q_{f,s}$ will vary around the value 1 and is comparable within species, but not among

296   species (unlike $R_{f,s}$).

297

298   7. Simulations

299   We performed two sets of simulations. The "abundance-specified simulation study"

300   demonstrates how well occupancy probabilities, abundance per subsample and other

301   variables (e.g. detection probabilities and relative abundances) can be estimated. The

302 "occupancy dynamics-focused simulation study" presents the sampling regimes under which

303 we might plausibly detect occupancy probability dynamics (i.e. non-overlapping 95%

304 credibility intervals) when the parameters were as estimated in our empirical data.

305   The simulated data of the abundance-specified simulation study was generated by

306 specifying the $\Psi_{f,s}'s$ and $\lambda_{f,s}'s$. Eqn. 7 was used for back-transforming into detection

307 probabilities and the data was then generated using Eqn. 3. We let species 1 have dynamics in

308 Ψ and species 2 have dynamics in λ.

309   For the occupancy dynamics-focused simulation study, we generated data under

310 different sampling intensisites (10, 20, 30, 50, 100 and 1000 sites per formation and 60, 100,

311 200, 400 and 1000 shells per site) and analyzed these data using the model and parameter

312 estimates from our empirical data. See SI for more details on both sets of simulations.

313

314 **Results**

315 *Empirical findings*

316 We found that including both the time-interval-dependent (Eqn 5) and the time-interval- and

317 species-dependent random effects (Eqn 6) improved the description of our empirical data (SI

318 Table S2). In other words, the full model (Eqn 6, illustrated in Fig. 2) was preferred over

319 simpler models, based on Bayes Factors (see the SI section on "MCMC for statistical

320 inference" for details), implying that the occupancy and detectability of the different

321 bryozoan species varied significantly with time-intervals (formation). However, including

322 paleoclimate explanatory variables or auto-correlated random effects did not improve our

323 model (SI Table S2). In other words, for our current data, we are not able to predict relative

324 abundance for unmeasured time-intervals beyond the median. The Bayes Factor did not

325 resolve the choice between the alternative "abundance-focused model" and Eqn 6, and the

326 models gave highly similar estimates of relative species abundances (see SI Fig. S4).

327   The overdispersion parameters, κ_s, were estimated to 0.09, 0.05, 0.04 and 0.07 for

328   *Antharcthoa tongima*, *Escharoides excavata* and *Arachnopusia unicornis* and the

329   superspecies, respectively (see Table S3 for credibility bands), where $\kappa_s = 0$ means no

330   overdispersion. While these estimates are close to zero, they represent overdispersion that

331   effectively doubles the variance, compared to no overdispersion (see SI Fig. S5).

332   The standard deviation parameters of the random effects have large uncertainty (Table

333   S3), except for the formation-dependent but species-independent random effect (σ_u) used for

334   detection probability. However, the model testing suggests that all random effects were

335   necessary to obtain an acceptable model fit.

336   The uncertainty surrounding the occupancy probability of each of the focal species is

337   quite large (Fig. 3), where we cannot establish that occupancy is well below 1.0 for any

338   combination of species and formation. Note that the relative changes in modelled detection

339   probabilities (Fig. 3) are similar to the dynamics of detection ratios (Fig. S2).

340   The relative species abundance (RSA; $R_{f,s}$) of the superspecies and *A. tongima* are

341   estimated with relatively high precision and vary significantly over time, while that of *E.*

342   *excavata* and *A. unicornis* are estimated with greater uncertainty (Fig. 4, see SI Figs. S4 and

343   S10 for alternative RSA's). The relative population density (RPD; $Q_{f,s}$) estimates (Fig. 5) are

344   also fairly uncertain, but some patterns are evident. Although the RSA of the superspecies

345   fluctuates noticeably over time (Fig. 4), its RPD is remarkably constant (Fig. 5). This

346   suggests that even though the abundance of single species may fluctuate substantially over

347   long time-scales, the abundance of the bryozoan community is rather stable, at least during

348   the time frame of this study (spanning c. 2 million years). Note that *A. tongima* and *E.*

349   *excavata* are about equally abundant in the oldest formations (Fig. 4), but *E. excavata*

350   becomes noticeably less abundant in the younger formations, at least relative to its own

351 average abundance over time (Fig. 5). The abundance of *A. unicornis* is reduced from the first

352 to the second time interval, and then remains relatively low.

353

354 *Simulation results*

355   The abundance-specified simulation study shows a spread of the estimates around the

356 true values for input parameters (SI Figs. S11-14) and the quantities that in our modelling are

357 derived, namely occupancy probabilities (SI Fig. S15), detection probabilities (SI Fig. S16)

358 and relative species abundances (Fig. 6). These estimates are spread quite evenly around both

359 sides of the actual values. Minute biases were expected (and found) given our informative

360 priors and non-linear transformations, but not cause for worry (see "abundance-specified

361 simulation study" in SI).

362   The occupancy dynamics-focused simulation study was designed for investigate if

363 sampling strategies can be improved for the same focal species and region. This simulation

364 indicated that occupancy dynamics are challenging to detect given our chosen species (see

365 "occupancy dynamics-focused simulation study" in SI for details).

366

367 **Discussion**

368 Ecologists are interested in estimating changing relative species abundance (RSA) and

369 population density (RPD) because it is a prime window into population dynamics (Sutherland

370 *et al.* 2013). On a shorter time scale, understanding how environmental attributes and species

371 traits affect population changes within communities are not only key to ecological

372 understanding but also conservation management (Bowler *et al.* 2018). On a longer time

373 scale, the changing of the relative abundance of fossil taxa have, in addition to acting as a

374 baseline for conservation (Barnosky *et al.* 2017), the potential for supplying direct

375 information on the evolution of phenotypes (Hannisdal 2006) and changing ecological

376   interactions (e.g. Liow *et al.* 2019) to enable linking paleoecological dynamics to

377   evolutionary changes. However, estimating numbers of individuals in nature is challenging,

378   regardless of the characteristics of organism (e.g. sessile or motile, small-bodied or large-

379   bodied), the type of data (e.g. direct counts, capture-recapture data), or the time-scale

380   involved (e.g. seasonal, yearly or paleoecological data). Occupancy modeling, which

381   explicitly models detection probabilities when estimating parameters of biological interest,

382   including changes in relative abundance, is one powerful way of incorporating different

383   sources of data heterogeneity and uncertainty. While occupancy modeling is increasingly

384   widespread in "traditional" ecological studies (Bailey et al. 2013), is yet to be applied

385   regularly in paleoecology. We believe our modelling framework has broad applicability e.g.

386   among lake or deep-sea drill cores and fossil outcrops where subsamples within sites can be

387   surveyed, and where relative species/taxon abundance rather than taxon richness is of

388   interest.

389   To briefly elaborate on the applicability of our modelling framework in

390   paleoecological settings, we emphasize that fossil detection probability is far from one, not

391   least because preservation is far from guaranteed (Kidwell & Holland 2002). Traditionally in

392   paleoecology, however, there is an underlying assumption, usually implicit, that preservation

393   (and hence the detection of preserved organisms) is comparable across samples and sites,

394   sometimes even across time-intervals, as long as sampling is standardized. Here, detection

395   ratios (see Methods: Study System) are usually presented as estimates of RSA (Kidwell 2002;

396   Currano *et al.* 2008; Espinosa *et al.* 2020). However, we know from simulations and

397   ecological studies that this assumption is problematic (Iknayan *et al.* 2014; MacKenzie *et al.*

398   2017). Not only is it important to progress beyond tabulations of paleoecological data for

399   improved inferences, parameters estimated using fossil data should be as comparable as

400   possible with the those estimated using living organisms. This will allow us to infer historical

401   baselines for conservation applications and to gain a better understanding of changing biota

402   over longer timescales for which we may have analogue crisis situations (Harnik *et al.* 2012;

403   Barnosky *et al.* 2017).

404   Instead of using the observed detection or non-detection of species, we could have

405   instead used the counts of the number of individuals of a given species in each subsample. If

406   we used the latter, we would have built a model similar to an N-mixture model (Royle 2004).

407   However, the subsamples in our example (shells or fragments thereof) varied in size and

408   these differences are expected to affect the number of individuals (colonies in our case). As

409   shell size was not quantified, a random effect for subsamples would be needed to account for

410   this variation. This inclusion would massively increase model complexity while introducing

411   an uncertainty that would make the extra information (counts per subsample in our case) of

412   little use. Since the computational cost would dramatically increase while the outcome was

413   not expected to improve significantly, we decided against this route for our empirical

414   demonstration. However, in other applications, subsample size can be accounted for.

415   The accuracy of the RSA and RPD estimates depends on how close the assumptions

416   concerning the proportionality coefficients are to reality. The estimates of RSA assume that

417   the proportionality coefficients do not vary among species, and the estimates of RPD assume

418   that the coefficients do not vary among formations for each species (i.e., both RSA and RPD

419   are only accurate at the same time if the proportionality coefficients are constant across both

420   species and formations). Our estimates of RSA apply only to the shell substrates that we have

421   sampled; likewise the unit for our RPD is density per shell. Hence, if it is desirable to

422   interpret the estimates given a different unit (e.g. per area sea bottom), one would have to

423   make additional assumptions. Such assumptions depend on the application. For our data, the

424   recruitment of encrusting bryozoans to substrates is thought to be largely limited by the

425   availability of adults, although substrate orientation, the presence of biofilms and substrate

426   types (e.g. hard substrates versus soft substrates like sea grass or kelp) may also influence

427   larval attachment and subsequent growth (Taylor & Wilson 2003) and may have species

428   specificity. We have purposefully limited our data collection to bivalve shells, the most

429   abundantly available and preserved substrate, which is always represented in our Pleistocene

430   system (Beu 2012). In addition, while bryozoans might be selective of habitats, e.g. the

431   strength of currents, coarse of sediments in the habitat affects their filter-feeding abilities,

432   (Wood *et al.* 2013) the same bryozoan species can be found on varied substrates, i.e. different

433   species of bivalves, rocks, gastropods and echinoderms (Rust & Gordon 2011). This

434   empirical knowledge encouraged us to estimate RPD ($Q_{f,s}$) assuming that the availability of

435   suitable substrate for any bryozoan species in our dataset is not limiting.

436   When estimating RPD, we removed the formation-specific random effects on

437   detection probability belonging to all species. This has a strong impact on the RPD estimates

438   since the standard deviations of these random effects are estimated to be quite substantial.

439   This random component is probably mostly reflecting variation in preservation in our study

440   system with similar bryozoan species encrusting the same shells. In other applications,

441   however, the time-specific random effects may reflect true fluctuations in the community

442   level abundance, and hence should not be removed.

443   One lesson learnt from our empirical modelling is that while we are able to estimate

444   the dynamics of relative species abundance (Fig. 4) and relative population density (Fig. 5),

445   the dynamics of occupancy are challenging to grasp in our empirical system. For our study,

446   the biggest driver of relative abundance is the dynamics of detection and thus of average

447   observable abundance per subsample given occupancy, while inferred occupancy probability

448   and its estimated uncertainty are estimated to be quite high for all species and formations,

449   thus revealing little dynamics (Fig. 3). This is because site-observations are high for all three

450   focal species even though subsample detection probabilities are relatively low. The

451   occupancy dynamics-focused simulations study showed that reliably getting occupancy

452   estimates that vary from formation to formation requires unfeasibly intense sampling

453   protocols for our choice of species, with the possible exception of *Escharoides excavata*.

454   Luckily, detecting occupancy dynamics was not the primary goal of the study, but in studies

455   where this is of principal concern, such issues should be considered before extensive data

456   collection.

457   We note several extensions to our models that can be considered, with regards to our

458   empirical system. First, other sources of system-specific variation might be taken into

459   account. In our example this includes the species of the shell substrate (e.g. some were

460   cockles and others were scallops) and their body size, both of which may be selected by the

461   bryozoan species involved and/or preferentially preserved. Second, we could potentially

462   handle the number of colonies of each species observed for each subsample, since this could

463   give an extra indication of the local average abundance per shell, although this is demanding

464   data collection-wise as well as computationally for our dataset (as mentioned in the paragraph

465   above). Third, in typical paleontological datasets, there are often time intervals in which we

466   are not able to sample fossils because suitable material was not deposited. In our empirical

467   example, we used two paleoenvironmental proxies ($\partial^{18}O$ and Mg/Ca ratios) as covariates in

468   expanded models (SI) in hope that they contained predictive information we could use on

469   unsampled time-intervals. While neither of the two we had published data for were

470   informative, it is possible that other paleoevironmental proxies given other paleoecological

471   occupancy datasets, could be explored for this purpose.

472   We hope that more paleoecologists will consider occupancy modeling as a means to

473   estimate relevant ecological parameters and that modelers will pick up where we left off to

474   improve the inference of biologically relevant parameters using a challenging but rich fossil

475   record.

476 **Code**

477 The code and data for all analyses are provided at

478 https://github.com/trondreitan/TRAMPOline

479 The name of the code package is called TRAMPOline based on an earlier acronym for the

480 project, Temporal Relative Abundance-focused multi-sPecies Occupancy model.

481

488
489

490 **References**

491 Barnosky, A.D., Hadly, E.A., Gonzalez, P., Head, J., Polly, P.D., Lawing, A.M., *et al.* (2017).

492   Merging paleobiology with conservation biology to guide the future of terrestrial

493   ecosystems. *Science*, 355.

494 Behrensmeyer, A.K., Kidwell, S.M. & Gastaldo, R.A. (2000). Taphonomy and paleobiology.

495   *Paleobiology*, 26, 103–147.

496 Bowler, D.E., Heldbjerg, H., Fox, A.D., O'Hara, R.B. & Böhning-Gaese, K. (2018).

497   Disentangling the effects of multiple environmental drivers on population changes

498   within communities. *J. Anim. Ecol.*, 87, 1034–1045.

499 Carter, R.M. & Naish, T.R. (1998). A review of Wanganui Basin, New Zealand: global

500   reference section for shallow marine, Plio-Pleistocene (2.5-0 Ma) cyclostratigraphy.

501   *Sediment. Geol.*, 122, 37–52.

502   Caswell, H. (2001). *Matrix Population Models; Construction, Analysis and Interpretation*.

503   Sinauer Associates, Sunderland, Massachusetts, U.S.A.

504   Currano, E.D., Wilf, P., Wing, S.L., Labandeira, C.C., Lovelock, E.C. & Royer, D.L. (2008).

505   Sharply increased insect herbivory during the Paleocene-Eocene Thermal Maximum.

506   *Proc. Natl. Acad. Sci.*, 105, 1960–1964.

507   Devarajan, K., Morelli, T.L. & Tenan, S. (2020). Multi-species occupancy models: review,

508   roadmap, and recommendations. *Ecography (Cop.).*, 43, 1612–1624.

509   Dorazio, R.M., Royle, J.A., Soderstrom, B. & Glimskar, A. (2006). Estimating species

510   richness and accumulation by modeling species occurrence and detectability. *Ecology*,

511   87, 842–854.

512   Espinosa, B.S., D'Apolito, C., Silva-Caminha, S.A.F., Ferreira, M.G. & Absy, M.L. (2020).

513   Neogene paleoecology and biogeography of a Malvoid pollen in northwestern South

514   America. *Rev. Palaeobot. Palynol.*, 273.

515   Fisher, R.A., Corbet, A.S. & Williams, C.B. (1943). The Relation Between the Number of

516   Species and the Number of Individuals in a Random Sample of an Animal Population. *J.*

517   *Anim. Ecol.*, 12, 42–58.

518   Hannisdal, B. (2006). Phenotypic Evolution in the Fossil Record: Numerical Experiments. *J.*

519   *Geol.*, 114, 133–153.

520   Harnik, P.G., Lotze, H.K., Anderson, S.C., Byrnes, J.E., Finkel, Z. V, Finnegan, S., *et al.*

521   (2012). Extinctions in ancient and modern seas. *Trends Ecol. Evol.*, 27, 608–617.

522   Iknayan, K.J., Tingley, M.W., Furnas, B.J. & Beissinger, S.R. (2014). Detecting diversity:

523   emerging methods to estimate species diversity. *Trends Ecol. Evol.*, 29, 97–106.

524   Jeffreys, H. (1998). *The Theory of Probability*. 3rd edn. Oxford University Pres.

525   Kidwell, S.M. (2002). Time-averaged molluscan death assemblages: Palimpsests of richness,

526   snapshots of abundance. *Geology*, 30, 803–806.

527   Kidwell, S.M. & Holland, S.M. (2002). The quality of the fossil record: Implications for

528   evolutionary analyses. *Annu. Rev. Ecol. Syst.*, 33, 561–588.

529   King, R. (2014). Statistical Ecology. *Annu. Rev. Stat. Its Appl.*, 1, 401–426.

530   Liow, L.H. (2013). Simultaneous estimation of occupancy and detection probabilities: an

531   illustration using Cincinnatian brachiopods. *Paleobiology*, 39, 193–213.

532   Liow, L.H., Reitan, T., Voje, K.L., Taylor, P.D. & Di Martino, E. (2019). Size, weapons, and

533   armor as predictors of competitive outcomes in fossil and contemporary marine

534   communities. *Ecol. Monogr.*, 89, e01354.

535   Lisiecki, L.E. & Raymo, M.E. (2005). A Pliocene-Pleistocene stack of 57 globally distributed

536   benthic δ18O records. *Paleoceanography*, 20, PA1003.

537   MacArthur, R.H. & Wilson, E.O. (1967). *The Theory of Island Biogeography*. *Monogr.*

538   *Popul. Biol.* Princeton University Press, Princeton, New Jersey.

539   MacKenzie, D., Nichols, J., Royle, A., Pollock, K., Bailey, L. & Hines, J. (2017). *Occupancy*

540   *Estimation and Modeling: Inferring Patterns and Dynamics of Species Occurrence.*

541   Academic Press.

542   MacKenzie, D.I., Nichols, J.D., Lachman, G.B., Droege, S., Andrew Royle, J. & Langtimm,

543   C.A. (2002). Estimating site occupancy rates when detection probabilities are less than

544   one. *Ecology*, 83, 2248–2255.

545   Pillans, B. (2017). Quaternary stratigraphy of Whanganui Basin—a globally significant

546   archive. In: *Landscape and Quaternary Environmental Change in New Zealand* (ed.

547   Shulmeister, J.). Atlantis Press, Paris, pp. 141–170.

548   Proust, J.N., Lamarche, G., Nodder, S. & Kamp, P.J. (2005). Sedimentary architecture of a

549   Plio-Pleistocene proto-back-arc basin: Wanganui Basin, New Zealand. *Sediment. Geol.*,

550   181, 107–145.

551   Royama, T. (1992). *Analytical Population Dynamics*. Chapman & Hall, London.

552   Royle, J.A. (2004). N-Mixture models for eestimating population size from spatially

553   replicated counts. *Biometrics*, 60, 108–115.

554   Royle, J.A. & Nichols, J.D. (2003). Estimating abundance from repeated presence-absence

555   data or point counts. *Ecology*, 84, 777–790.

556   Schwarz, C.J. & Seber, G.A.F. (1999). Estimating animal abundance: review III. *Stat. Sci.*,

557   14, 427–456.

558   Sosdian, S. & Rosenthal, Y. (2009). Deep-sea semperature and ice volume changes ccross the

559   Pliocene-Pleistocene climate transitions. *Science (80-.).*, 325, 306 LP – 310.

560   Sutherland, W.J., Freckleton, R.P., Godfray, H.C.J., Beissinger, S.R., Benton, T., Cameron,

561   D.D., *et al.* (2013). Identification of 100 fundamental ecological questions. *J. Ecol.*, 101,

562   58–67.

563   Williams, B.K., Nichols, J. & Conroy, M.J. (2002). *Analysis and Management of Animal*

564   *Populations*. Academic Press, San Diego, San Francisco, New York, Boston, London,

565   Sydney, Tokyo.

566   Yamaura, Y., Andrew Royle, J., Kuboi, K., Tada, T., Ikeno, S. & Makino, S. (2011).

567   Modelling community dynamics based on species-level abundance models from

568   detection/nondetection data. *J. Appl. Ecol.*, 48, 67–75.

569   Zipkin, E.F., Andrew Royle, J., Dawson, D.K. & Bates, S. (2010). Multi-species occurrence

570   models to evaluate the effects of conservation and management actions. *Biol. Conserv.*,

571   143, 479–484.

572

Figure captions

Figure 1: A schematic diagram to show the sampling scheme. Each thick bordered open rectangle represents a time-interval (two are illustrated more fully, the first time-interval, T1, and the nth time-interval, Tn). Within each time-interval, Sites (dotted rectangles) are sampled (two are more fully illustrated in each). Within each site, there are subsamples (smaller, solid bordered rectangles) in which different species (solid shapes) are observed. The open circle can represent a superspecies (see main text), which in our example is assumed to be present in all sites, even if unsampled.

Figure 2. Full hierarchical occupancy model to estimate relative abundance. This figure summarizes our full hierarchical occupancy model for estimating relative abundane (RSA or RPD) composed of top level parameters and random effects that describe their overdispersion. Data are denoted as triangles where N are the number of sites and y the shells from site i where species s is observed. Black circles denote occupancy parameters, white circles denote detection parameters and grey circle denotes the overdispersion parameter. An arrow from an element A (i.e. circle, triangle or rectangle) to another B, denotes that B is conditioned on A either by a function or a distribution (see text for details).
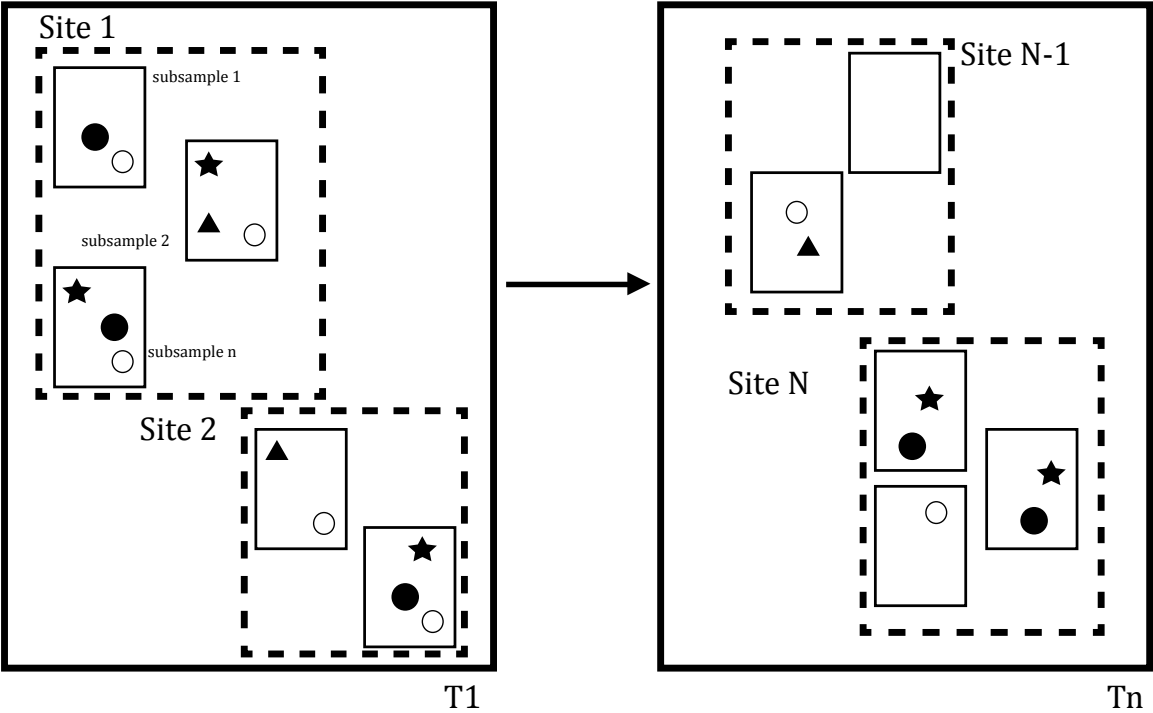

Figure 3. Estimated occupancy and detection probabilities. Estimates are from our full model where black lines join the species posterior median occupancy for each formation (time-interval) plotted in the middle of the age range of the given formation. Grey lines show 95% posterior credibility intervals for the estimates. Note that the occupancy for superspecies is not plotted as it is assumed to be 1 throughout and that the y-axes for occupancy and detection are different.

Figure 4: Estimated relative species abundance (RSA). Estimates are from our full model where black lines join the species mean relative species abundance, R, (plotted on a log scale, except for the superspecies for visibility) for each formation (time-interval). Grey lines show 95% posterior credibility intervals for the estimates and medians. A relative species abundance of 0.1 (for a given species in a time-interval given) means that every tenth bryozoan colony in the region was of this species. The inset on the right ("Combined") shows the estimates combined for the four species/superspecies from their separate plots (note the different scale used for visual clarity).

Figure 5: Estimated relative population density (RPD). Estimates are from our full model where black lines join the species mean relative population density, Q, for each formation (time-interval). Grey lines show 95% posterior credibility intervals for the estimates. Formation specific values are divided by the mean across formations. Hence, a value of 0.1 means that the abundance is 10% of the mean across formations for the given species (horizontal stippled lines at value 1)

Figure 6: Relative species abundances from the abundance-specified simulation study. Solid black lines show the true relative species abundances for the various species and formations, while the points are estimates from the 100 simulated datasets. We show estimates from 5 examples runs in each panel (light grey lines)

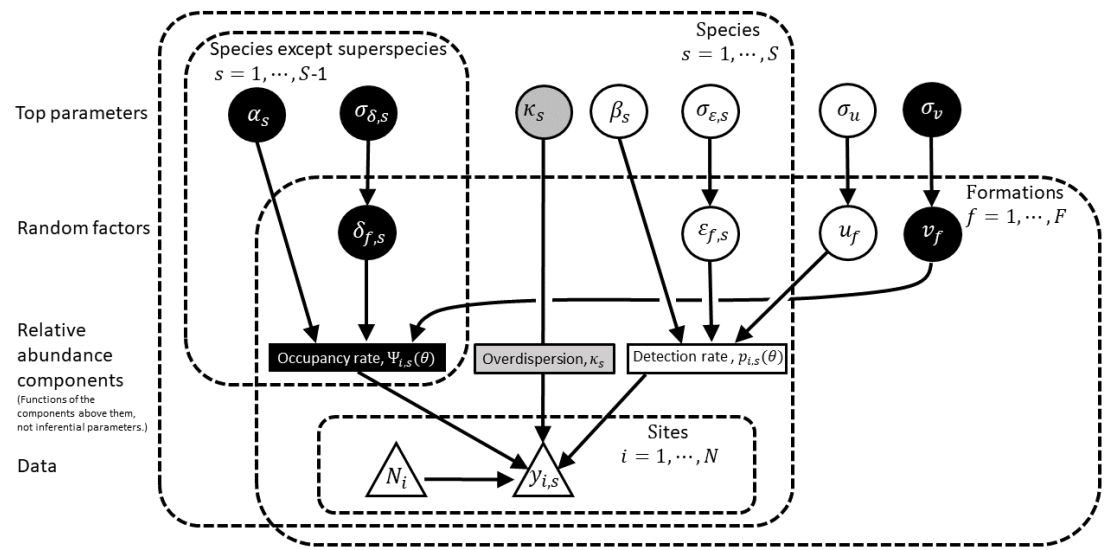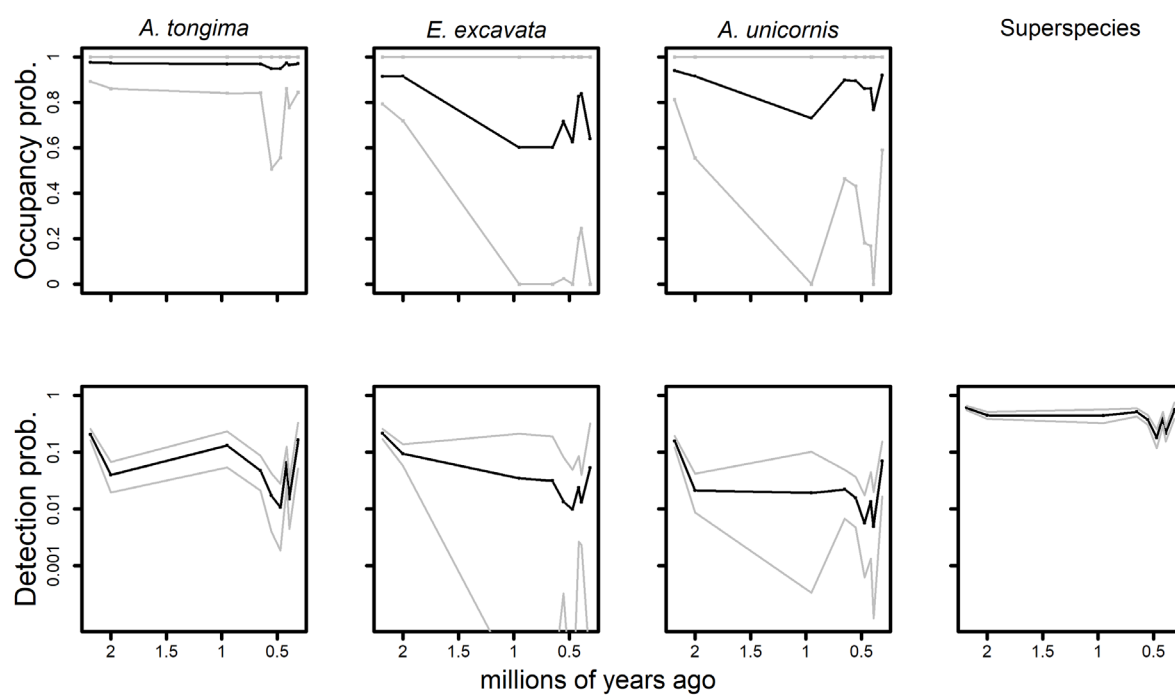617   **Figure 1: A schematic diagram to show the sampling scheme.**
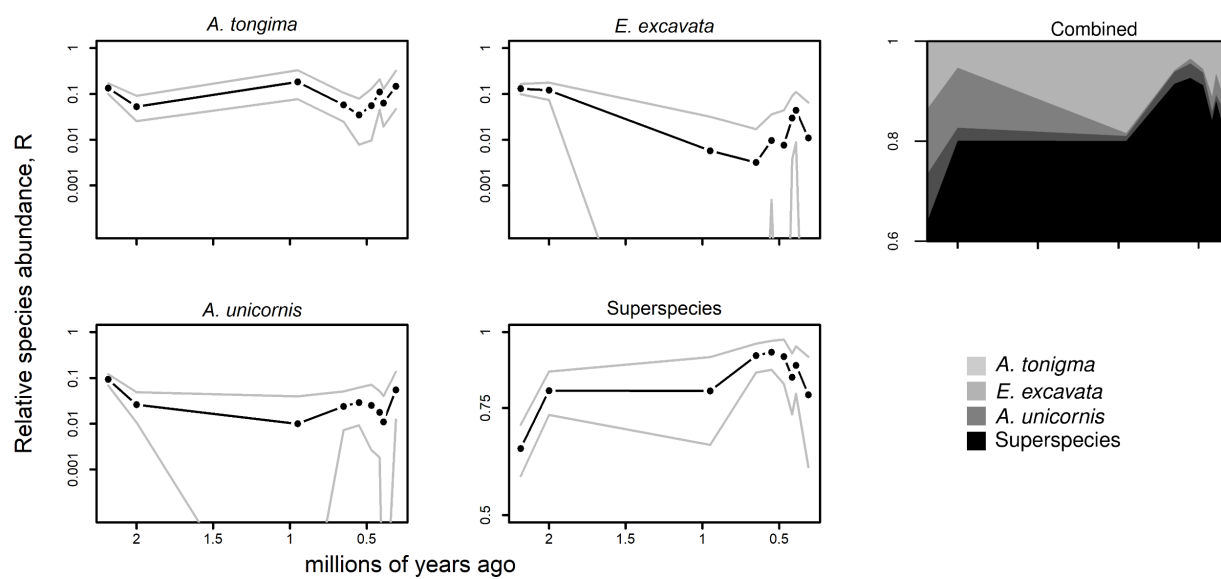

618

619

620

621   **Figure 2: Full hierarchical occupancy model to estimate relative abundance**
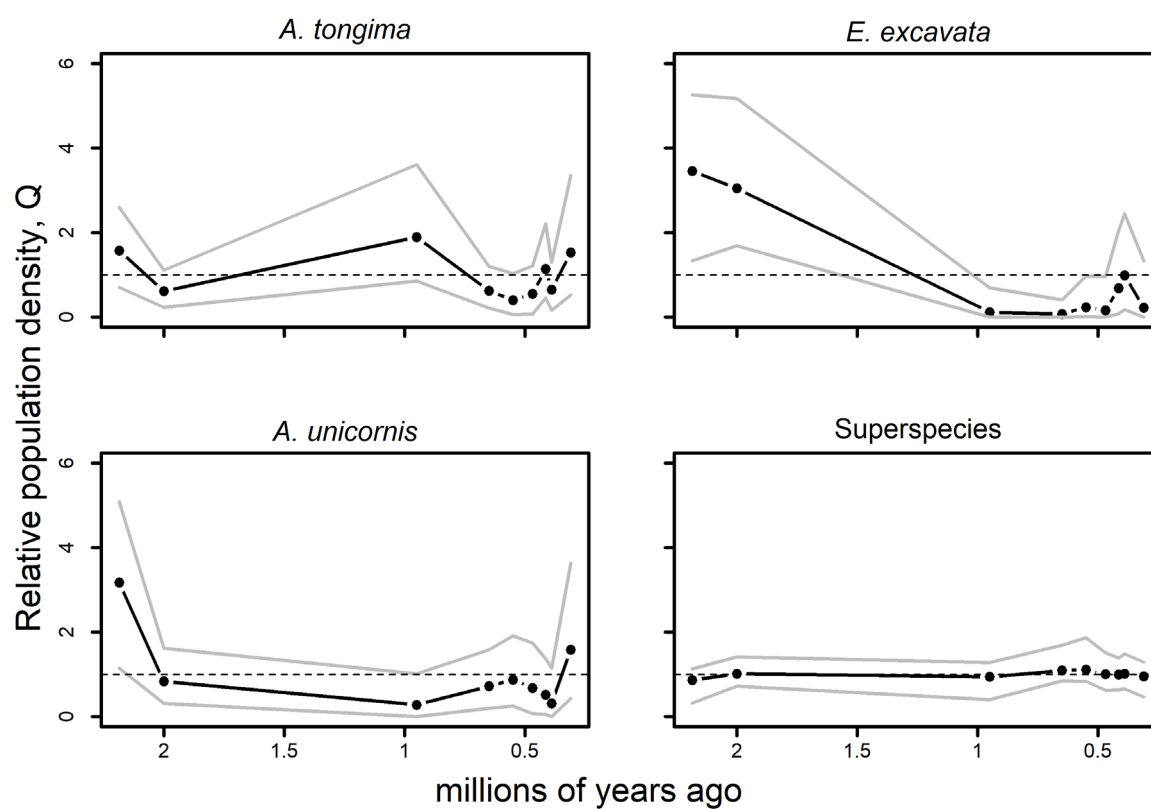

622

623

624

625   **Figure 3: Estimated occupancy and detection probabilities.**

626

627

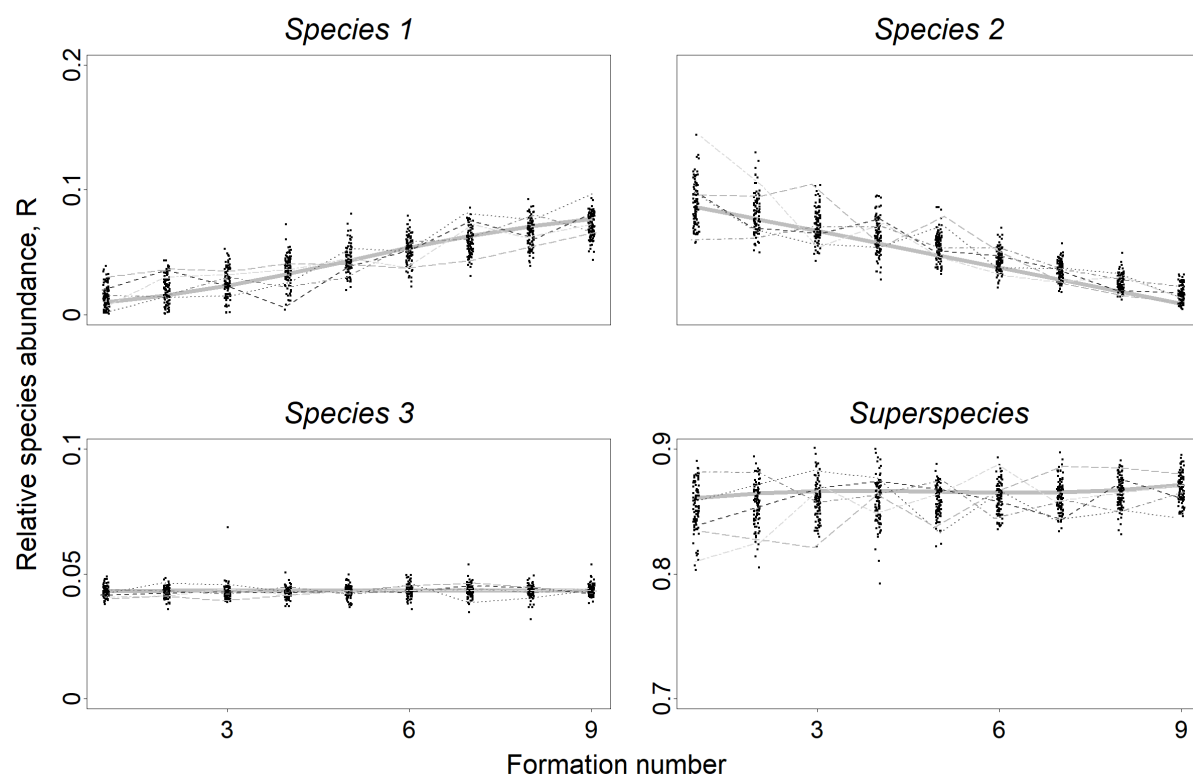**Figure 4. Estimated relative species abundance (RSA).**

631 **Figure 5: Estimated relative population density (RPD).**

632

633

Figure 6: Relative species abundances from the abundance-specified simulation study.

635